Long-time instability in the Runge-Kutta algorithm for a Nosé-Hoover heat bath of a harmonic chain and its stabilization

Baiyili Liu
College of Environment and Civil Engineering, Chengdu University of Technology, Chengdu 610059, China
and HEDPS and CAPT, College of Engineering, Peking University, Beijing 100871, China

Shaoqiang Tang*
HEDPS, CAPT, and LTCS, College of Engineering, Peking University, Beijing 100871, China
and IFSA Collaborative Innovation Center of MoE, Shanghai Jiaotong University, Shanghai, China
(Received 6 November 2016; revised manuscript received 12 June 2017; published 13 July 2017)

In this paper, we investigate the Runge-Kutta algorithm for the Nosé-Hoover heat bath of a harmonic chain. The Runge-Kutta algorithm is found to be unstable in long-time calculations, with the system temperature growing exponentially. The growth rate increases if time step size is chosen larger. By analyzing the Fourier spectra in both space (wave number) and time (frequency), we discover that the growth is caused by spurious energy accumulation, particularly at the largest wave number. Such accumulation may be explained by von Neumann analysis for an infinite chain, with the nonlinear heat bath being ignored. Furthermore, we propose to add a filter to remove excessive energy, which effectively stabilizes the algorithm.

DOI: 10.1103/PhysRevE.96.013308

I. INTRODUCTION

Nowadays, molecular dynamics simulations are indispensable in materials science and engineering. Two major components in the numerical computation are time integration and force calculation with a certain potential. As the physical properties and dynamics of materials heavily depend on temperature, it is vital in molecular dynamics simulation to design and implement faithful and efficient algorithms to incorporate finite temperature and thermal fluctuations.

Over the past several decades, there have been various heat baths (thermostats) invented to maintain finite temperature for an atomic lattice, such as those named after Anderson [1], Berendsen [2], Langevin [3], Nosé-Hoover [4,5], and more recently the phonon heat bath [6] and heat jet approach [7,8]. In the Nosé-Hoover heat bath, temperature is controlled through a feedback mechanism with additional auxiliary variables. It is widely used in both equilibrium statistic physics and nonequilibrium statistic physics, due to its nice physical properties [9], such as producing canonical ensembles and maintaining ergodicity.

Commonly used time integration algorithms for the Nosé-Hoover heat bath include the Runge-Kutta algorithm [10], the velocity verlet algorithm [11], the reversible reference system propagator algorithm (r-RESPA) [12], etc. The velocity verlet algorithm is symplectic when applied to a Hamiltonian system, and often used in heat transfer studies, such as thermal conductivity for the Fermi-Pasta-Ulam-β (FPU-β) atomic chain [13–17], Frenkel-Kontorova atomic chain [18], few-layer graphene [19], and carbon nanotube [20]. The r-RESPA is time reversal, and used for the Nosé-Hoover heat bath to control temperature in constant-temperature atomic simulations [21–23]. Although the Runge-Kutta algorithm is neither symplectic nor time reversal, it is still widely used to integrate the Nosé-Hoover heat bath to explore thermal conductivity for a nonlinear chain, such as the FPU-β atomic chain [13,24–29], Frenkel-Kontorova atomic chain [30,31], ϕ^4 potential lattice [31], Toda lattice [32], and on-site potential lattice [33]. Moreover, the Runge-Kutta algorithm is the dominant integrator for ordinary differential equations, and handy in dealing with nonequilibrium simulations, such as crack tip motion under finite temperature. As a matter of fact, stability concerns on the Runge-Kutta method for a harmonic oscillator triggered the study of symplectic algorithms three decades ago, starting with the seminal work of Feng [34]. Some symplectic Runge-Kutta algorithms have been developed since then [35,36], yet stability of the Runge-Kutta algorithm for the Nosé-Hoover heat bath of a linear harmonic chain has not yet been well explored. Furthermore, the commonly used form of the Nosé-Hoover heat bath is not a Hamiltonian system.

This paper is motivated by comparison of the Runge-Kutta algorithm and the velocity verlet algorithm for the Nosé-Hoover heat bath. No meaningful difference between them appears in numerical tests for an anharmonic chain. However, when a linear harmonic chain is under consideration, quite unexpectedly they lead to totally different simulation results. While the velocity verlet algorithm provides desired uniform temperature distribution and correct spectrum, the Runge-Kutta algorithm, as we shall describe later on, produces indefinitely growing temperature and abnormal spectra. The Runge-Kutta algorithm is known to be an explicit scheme, hence it has a restriction of time step size to maintain stability in general [37]. Yet this does not explain the numerical observation of instability, which always presents in a long enough run, regardless of how fine a time step size one chooses. This motivates a substantial exploration for stability (long-time instability) in the Runge-Kutta algorithm for the Nosé-Hoover heat bath of a harmonic chain.

Through a standard von Neumann analysis for an infinite harmonic chain, with the nonlinear heat bath being ignored, each normal mode is found unstable. The amplification factor depends on both the time step size and the wave number. More precisely, instability diminishes along with

*maotang@pku.edu.cn

refinement of time discretization, and short waves grow faster.

Now consider a finite harmonic chain. The contact with the Nosé-Hoover heat bath brings in nonlinearity. Numerical evidences suggest that the linear stability analysis captures the main mechanism in the nonlinear system, e.g., instability occurs earlier and more severe at a larger time step size. Moreover, the wave number spectrum and frequency spectrum analyses reveal that the temperature growth is heavily related to the spurious energy accumulation at the largest wave number.

For a nonlinear chain with the Nosé-Hoover heat bath, strong nonlinearity blends different modes, and the feedback mechanism in the heat bath stabilizes the whole system. Therefore, the Runge-Kutta algorithm appears stable for long-time integration. In contrast, when applied to the linear harmonic chain, nonlinearity only appears in the heat bath. It is not enough to blend the energy among different modes, and leads to indefinite growth of temperature.

With the above understanding, the Runge-Kutta algorithm may be remedied by a straightforward stabilization. We introduce a filter to remove excessive energy at large wave numbers after every fixed time period (filtering time). The influence and choice of this empirical filtering time are investigated by numerical tests. When it is suitably chosen, the stabilized Runge-Kutta algorithm yields normal temperature and spectra. The effective stabilization of this filtering method, in turn, justifies our explanation of the long-time instability.

We remark that while it is debatable whether the Nosé-Hoover heat bath is suitable for the harmonic chain, better understanding of the numerical integration algorithm may lay a solid foundation for faithful simulation tools.

The rest of this paper is organized as follows. In Sec. II, we describe the governing equations of a linear harmonic lattice under the Nosé-Hoover heat bath, the Runge-Kutta algorithm for time integration, as well as von Neumann stability analysis for an infinite harmonic chain. In Sec. III, we present numerical simulation results and data analysis. In Sec. IV, a stabilized algorithm is proposed and tested numerically. Finally, we make some concluding remarks in Sec. V.

II. MODEL, NUMERICAL ALGORITHM, AND LINEAR STABILITY ANALYSIS

We consider a finite harmonic chain of N atoms with nearest neighboring interaction. A Nosé-Hoover heat bath is adopted for the boundary atoms at temperature T_L and T_R, respectively [25]. With $q_0 = q_{N+1} = 0$ and $f_n = q_{n-1} - 2q_n + q_{n+1}$, the dimensionless governing equations are

$$\ddot{q}_n = f_n, \quad n = 2,3,\ldots,N-1, \tag{1}$$

$$\ddot{q}_1 = f_1 - \zeta_L \dot{q}_1, \tag{2}$$

$$\ddot{q}_N = f_N - \zeta_R \dot{q}_N, \tag{3}$$

$$\dot{\zeta}_L = \frac{1}{\theta}\left(\frac{\dot{q}_1^2}{T_L} - 1\right), \tag{4}$$

$$\dot{\zeta}_R = \frac{1}{\theta}\left(\frac{\dot{q}_N^2}{T_R} - 1\right). \tag{5}$$

Here, q_n is the displacement of the nth atom away from its equilibrium, $\zeta_{L,R}$ are two auxiliary variables, and θ is an empirically chosen parameter representing coupling strength. From numerical simulations, we observe no obvious impact of the initial value of $\zeta_{L,R}$. Meanwhile, the impact of θ on heat bath has been explained in [24]. For definitiveness, we take $\zeta_{L,R}(0) = 1$ and $\theta = 1$ for all following numerical simulations.

Taking the first atom as an example, when its kinetic energy exceeds the applied temperature T_L, $\dot{\zeta}_L$ is greater than zero. Then ζ_L tends to increase to a positive value, and damps the kinetic energy of the first atom. On the other hand, when the kinetic energy is low, a negative damping term pumps in energy. Through this feedback mechanism, the kinetic energy is maintained around the applied temperature.

In this paper, we are mainly concerned with numerical integration for the system (1)–(5). The second order Runge-Kutta algorithm is adopted for time integration. More precisely, with a time step size h and notation

$$U = \begin{bmatrix} q_1 \\ q_2 \\ \vdots \\ q_{N-1} \\ q_N \\ \dot{q}_1 \\ \dot{q}_2 \\ \vdots \\ \dot{q}_{N-1} \\ \dot{q}_N \\ \zeta_L \\ \zeta_R \end{bmatrix}, \quad F(U) = \begin{bmatrix} \dot{q}_1 \\ \dot{q}_2 \\ \vdots \\ \dot{q}_{N-1} \\ \dot{q}_N \\ f_1 - \zeta_L \dot{q}_1 \\ f_2 \\ \vdots \\ f_{N-1} \\ f_N - \zeta_R \dot{q}_N \\ (\frac{q_1^2}{T_L} - 1)/\theta \\ (\frac{\dot{q}_N^2}{T_R} - 1)/\theta \end{bmatrix}, \tag{6}$$

the second order Runge-Kutta algorithm can be expressed as

$$U^* = U^p + hF(U^p), \tag{7}$$

$$U^{p+1} = U^p + \frac{h}{2}[F(U^p) + F(U^*)]. \tag{8}$$

To understand stability of the Runge-Kutta algorithm, we perform von Neumann stability analysis for the infinite harmonic chain (without the heat bath). We introduce $Q^p(\xi) = \frac{1}{\sqrt{2\pi}} \sum_n e^{-i\xi n} q_n^p$ to be the Fourier transform of the displacement. The Runge-Kutta algorithm leads to

$$Q^* = Q^p + h\dot{Q}^p, \tag{9}$$

$$\dot{Q}^* = \dot{Q}^p - h\omega^2 Q^p, \tag{10}$$

$$Q^{p+1} = Q^p + \frac{h}{2}(\dot{Q}^p + \dot{Q}^*), \tag{11}$$

$$\dot{Q}^{p+1} = \dot{Q}^p - \frac{h\omega^2}{2}(Q^p + Q^*). \tag{12}$$

Here, $\omega = 2\sin\frac{\xi}{2}$ is the dispersion relation. Eliminating Q^* and $\dot{Q}^*$, we have

$$\begin{bmatrix} Q^{p+1} \\ \dot{Q}^{p+1} \end{bmatrix} = \begin{bmatrix} 1 - \frac{h^2\omega^2}{2} & h \\ -h\omega^2 & 1 - \frac{h^2\omega^2}{2} \end{bmatrix} \begin{bmatrix} Q^p \\ \dot{Q}^p \end{bmatrix}. \tag{13}$$

The eigenvalues to the coefficient matrix are $\lambda = (1 - \frac{h^2\omega^2}{2}) \pm ih\omega$. The modulus $|\lambda| = \sqrt{1 + \frac{h^4\omega^4}{4}}$ is greater than 1, indicating instability of the Runge-Kutta algorithm. The energy of each mode increases exponentially as $|\lambda|^{2t/h}$, hence the growth rate is $\frac{1}{h}\log_{10}(1 + \frac{h^4\omega^4}{4})$. From this expression, energy grows fastest at the maximal frequency $\omega = 2$ or wave number $\xi = \pi$, with a growth rate $k_{\text{ref}} = \frac{1}{h}\log_{10}(1 + 4h^4)$. Furthermore, the growth rate decays toward zero if $h \to 0$. Hence, a smaller time step size is preferable for stability concerns.

We remark that the analysis is valid for the linear chain only. With the heat bath, the interplay between such instability and nonlinearity can be delicate. Careful numerical studies are hence carried out.

III. NUMERICAL RESULTS

In this section, we first introduce some definitions and notations. Then we display the temperature and spectrum for the Runge-Kutta algorithm, and illustrate the reason for temperature growth. Having gained an understanding, we further propose a stabilized Runge-Kutta algorithm.

We simulate a harmonic chain with $N = 256$ atoms at temperature $T_L = T_R = 10$. Time step size is chosen as $h = 0.01$, unless otherwise specified. We denote the total computation time as t_a, and a suitable truncation time as t_c.

A. Definitions and notations

Following [24], we define a time dependent system temperature:

$$T(t) = \frac{1}{N}\sum_{n=1}^{N}\dot{q}_n^2(t). \tag{14}$$

To compare with the theoretical growth rate k_{ref}, we define a time dependent growth rate of system temperature:

$$k(t_l) = \frac{\log_{10}\bar{T}(t_{l+1}) - \log_{10}\bar{T}(t_l)}{t_{l+1} - t_l}. \tag{15}$$

Here, $\bar{T}(t_l)$ represents the average of system temperatures for time t_l to t_{l+1}. The value of sampling time t_l is taken at regular intervals, and the choice is not unique. In numerical simulation, we take $t_l = \frac{l}{20}t_a$ $(l = 1,2,\ldots,20)$.

We further define a local temperature (average kinetic energy for the nth atom), when the system reaches the local equilibrium state:

$$T_n = \frac{1}{t_a - t_c}\int_{t_c}^{t_a}\dot{q}_n^2(\tau)d\tau. \tag{16}$$

We take the Fourier transform for velocity in space $A_{\xi,i} = |\mathcal{F}_{n\to\xi}\{\dot{q}_n(t_i)\}|, (i = 1,2,3,\ldots,I)$. Due to large fluctuations in the instantaneous amplitude $A_{\xi,i}$, we define a mean amplitude $A(\xi) = \frac{1}{I}\sum_{i=1}^{I}A_{\xi,i}$ as the time average of the instantaneous amplitudes. Here the wave number ξ takes discrete values from zero to π with an increment $\frac{2\pi}{N}$. The value of integer I should be large enough. In numerical simulations, we take the sampling time $t_i = \frac{i}{100}t_a$ $(l = 1,2,3,\ldots,100)$. Furthermore, we shall focus on $A_{\pi,i}$ to observe the evolution for the most unstable mode.

We also calculate the frequency spectrum near the termination time, and denote the amplitude $B(\omega) = |\mathcal{F}_{t\to\omega}\{\dot{q}_1(t)\}|$ with $t \in [t_a - 1\times10^4, t_a]$. To check energy change for the largest frequency $\omega = 2$, we define an instantaneous amplitude $B_{2,j} = |\mathcal{F}_{t_j\to\omega}\{\dot{q}_1(t_j)\}|$. The time t_j represents a period of time within $[\frac{t_a}{50}j - 1\times10^4, \frac{t_a}{50}j]$ $(j = 1,2,\ldots,50)$.

B. Long-time instability

We display simulation results with initial data $q_n(0) = (-1)^n$ and $\dot{q}_n(0) = 0$, corresponding to the most unstable mode $\xi = \pi$. We observe in Fig. 1(a) that the system temperature grows slowly in the beginning, and exponentially afterwards. The growing tendency is close to the solid line representing the theoretical growth rate for an infinite chain, yet at a different growth rate. In Fig. 1(b), the local temperatures of the interior atoms grow indefinitely, distributing in a parabola shape. Owing to the exponential growth, the amplitude of local temperature depends mainly on the last moment, while the shape stays the same.

The temperature growth may be analyzed from the wave number spectrum. See Fig. 1(c). The mean amplitude $A(\xi)$ does not distribute uniformly. Energy at the wave number $\xi = \pi$ grows fastest and makes the main contribution to the system temperature growth. This is consistent with theoretical analysis for the linear infinite chain. Other high frequency modes also grow and contribute. See Fig. 1(d). The instantaneous amplitude $A_\pi(t)$ does not fluctuate around a certain value. It grows exponentially with fluctuations. Comparing with Figs. 1(a) and 1(d), the growth rate of $A_\pi(t)$ is about half that of $T(t)$. Notice that $A_\pi(t)$ represents the growth of velocity, whereas $T(t)$ represents that of the square of velocity.

Despite the growth for the entire chain, the feedback mechanism of the heat bath maintains the local temperature T_1 and T_N at the applied temperature. From the frequency spectrum of the first atom in Fig. 1(e), the energy concentrates at the frequency $\omega = 2$. Other frequencies take rather small amplitudes. In Fig. 1(f), the instantaneous amplitude $B_2(t_j)$ gradually goes up and then keeps fluctuating around a certain value, consistent with a fixed T_1.

According to the linear stability analysis, the theoretical growth rate of the system temperature depends on the time step size h. For the nonlinear system with heat bath, we take a range of time step size from 0.05 to 0.006. When the time step size is small, it takes a long total computing time to observe growth for the system temperature. In Fig. 2, stars represent numerical growth rate $k(t_l)$ and solid lines represent theoretical growth rate k_{ref}. For time step size larger than 0.01, the numerical growth rates increase quickly and then maintain at the corresponding theoretical ones. It is similar for smaller time step sizes, though the logarithmic plotting makes an illusion of abrupt approaching. The larger time step size we take, the more quickly the numerical growth rate reaches the solid line.

For an even smaller time step size such as $h = 0.005$, the system temperature does not show observable growth even at $t = 5\times10^8$. See Fig. 3. It fluctuates around the applied temperature. Furthermore, the local temperature grows very slowly, and still forms a mild hump in the middle.

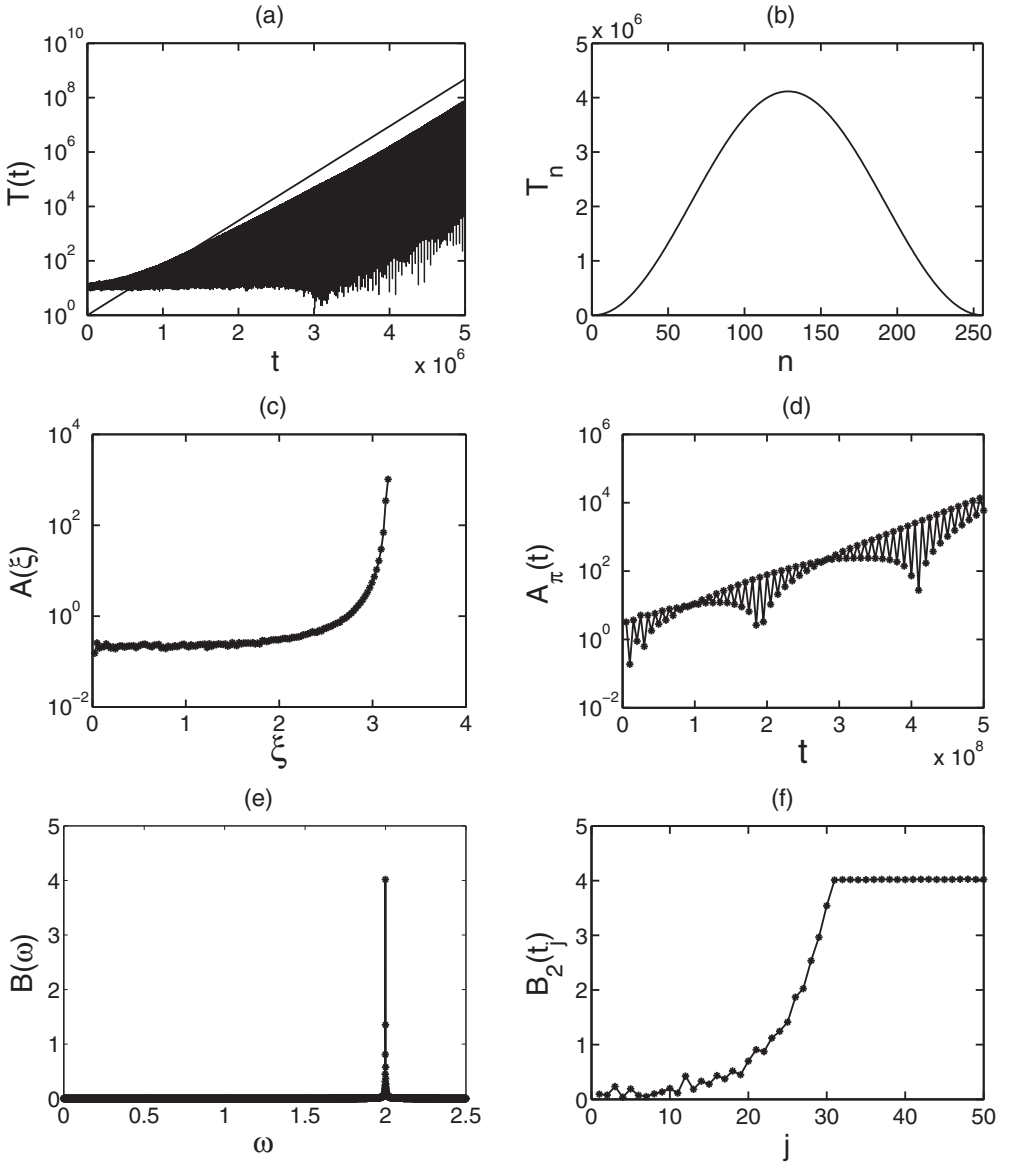

FIG. 1. Runge-Kutta algorithm with step size $h = 0.01$: (a) system temperature, (b) local temperature, (c) time average of wave number spectrum, (d) instantaneous wave number spectrum at $\xi = \pi$, (e) frequency spectrum, and (f) instantaneous frequency spectrum at $\omega = 2$.

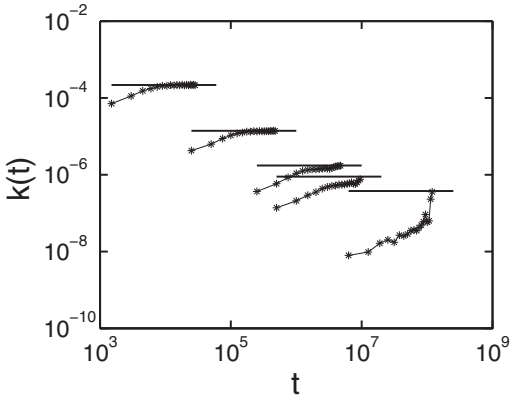

FIG. 2. Runge-Kutta algorithm with step size $h = 0.05, 0.02, 0.01, 0.008, 0.006$ from top to bottom. Stars represent numerical growth rate, and solid lines represent theoretical growth rate.

In the above, we discover that the system temperature growth is well expected from the linear stability analysis for the infinite chain. Energy of the most unstable mode $\xi = \pi$ grows fastest, again consistent with theoretical analysis.

It is worth mentioning that other initial conditions have also been tested. They only affect when the temperature shows an exponential growth, whereas the exponential growth rate is determined solely by the time step size.

IV. STABILIZED RUNGE-KUTTA ALGORITHM

In many applications, the Runge-Kutta algorithm is widely adopted for its convenience in coding and high accuracy. As the instability is mainly due to the accumulation of spurious energy at the most unstable wave number, we propose to add a filter to remove excessive energy at large wave numbers after every fixed time period Δt_f.

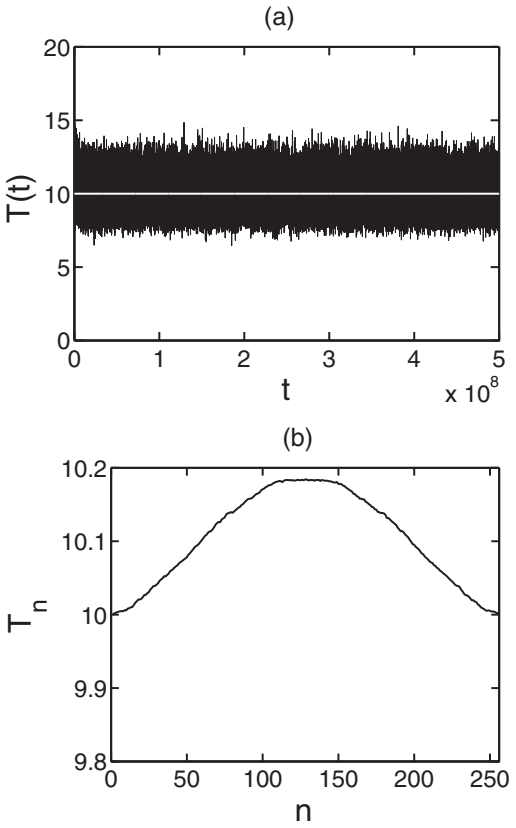

FIG. 3. Runge-Kutta algorithm with step size $h = 0.005$: (a) System temperature, (b) Local temperature.

More precisely, in view of the high amplitudes of the last four points in Fig. 1(c), we simply clear these modes with $\xi = \frac{125}{128}\pi, \frac{126}{128}\pi, \frac{127}{128}\pi, \pi$. Then we adopt a rectangular filter:

$$G(\xi) = \begin{cases} 1, & 0 \leqslant |\xi| < \frac{125}{128}\pi; \\ 0, & \frac{125}{128}\pi \leqslant |\xi| < \pi. \end{cases} \tag{17}$$

At time $t_\alpha = \alpha \cdot \Delta t_f$ ($\alpha = 1, 2, \ldots$), we insert a filtering step as follows:

$$\begin{aligned} q_n^*(t_\alpha) &= \mathcal{F}^{-1}_{\xi\to n}\{\mathcal{F}_{n\to\xi}\{q_n(t_\alpha)\} \cdot G(\xi)\}, \\ \dot{q}_n^*(t_\alpha) &= \mathcal{F}^{-1}_{\xi\to n}\{\mathcal{F}_{n\to\xi}\{\dot{q}_n(t_\alpha)\} G(\xi)\}. \end{aligned} \tag{18}$$

The filtering time Δt_f is an empirical parameter depending on the time step size. If the time step size is big, the high frequency modes grow quickly. Hence we choose a short filtering time. We illustrate the stabilized algorithm with initial data $q_n(0) = 1$ and $\dot{q}_n(0) = 0$, and time step size $h = 0.01$. We compute with $t = 8 \times 10^7$ and $\Delta t_f = 4 \times 10^5$.

After filtering, temperature profiles and spectrum are rectified. The system temperature does not grow exponentially anymore. See Fig. 4. It keeps fluctuating around the applied temperature. The filter causes relatively bigger temperature fluctuations. See Figs. 4(c) and 4(d). The mean amplitude of each mode $A(\xi)$ distributes uniformly around a certain value. For the most unstable mode, the instantaneous amplitude $A_\pi(t)$ does not rise indefinitely. This verifies the effectiveness of the filter in avoiding accumulation of energy at the most unstable mode.

To make comparison, we choose other filtering time Δt_f and check the local temperature and spectrum. See Figs. 5(a)

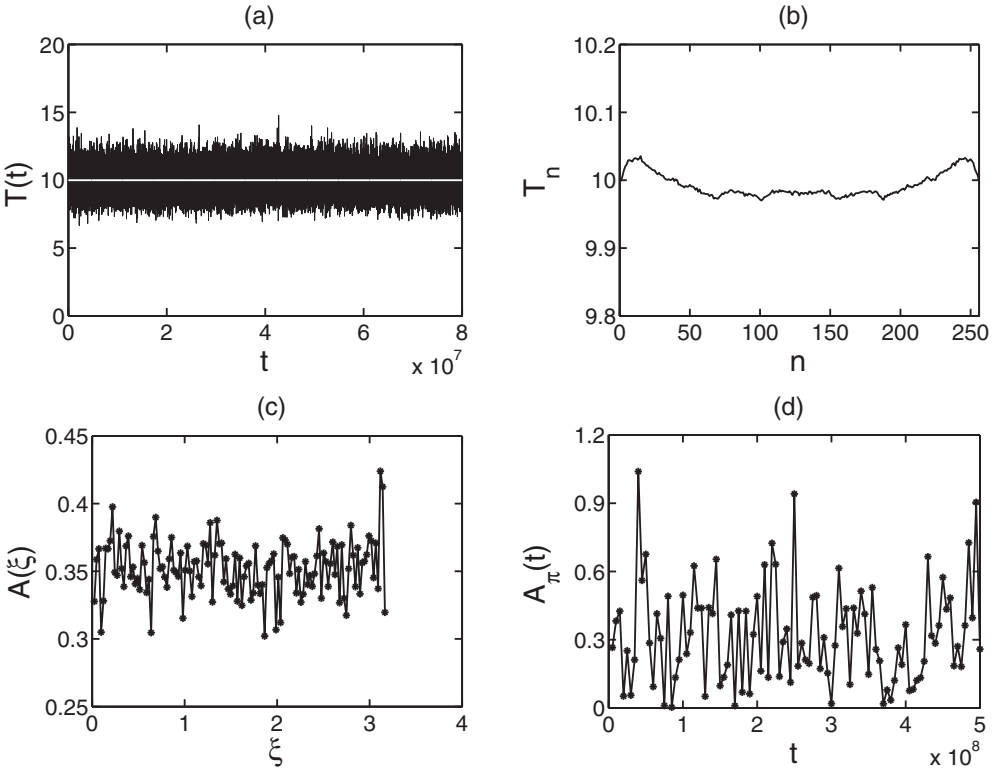

FIG. 4. The stabilized Runge-Kutta algorithm with a filtering time $\Delta t_f = 4 \times 10^5$: (a) system temperature, (b) local temperature, (c) time average of wave number spectrum, and (d) instantaneous wave number spectrum at $\xi = \pi$.

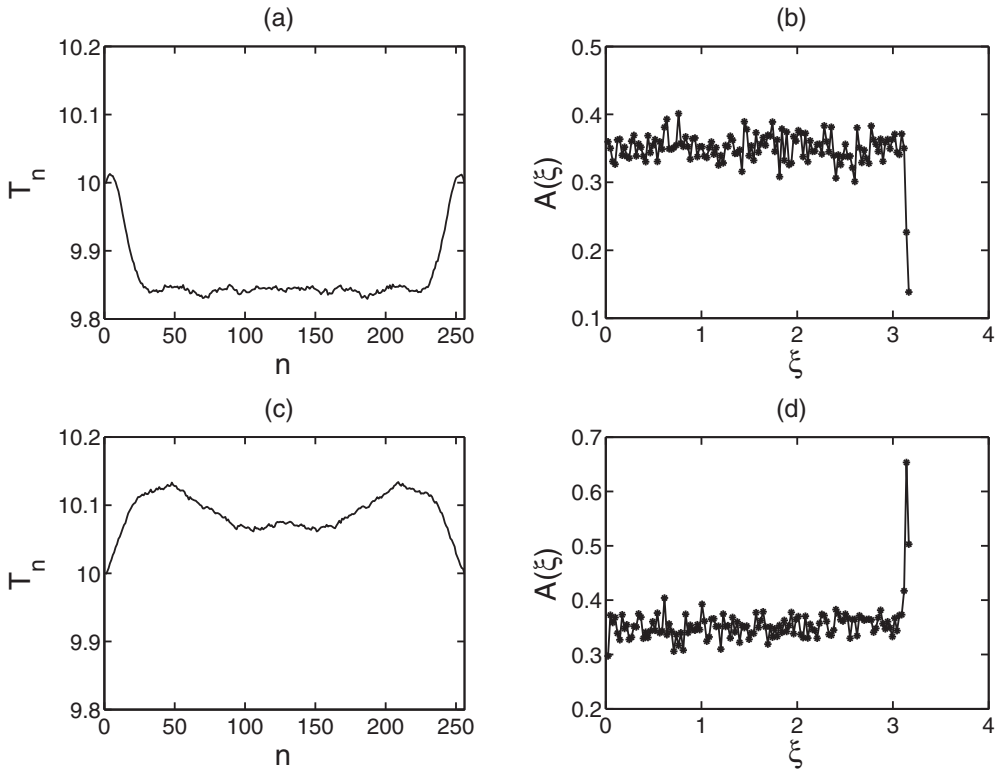

FIG. 5. The stabilized Runge-Kutta algorithm with different filtering time: (a) local temperature with $\Delta t_f = 1 \times 10^5$, (b) time average of wave number spectrum with $\Delta t_f = 1 \times 10^5$, (c) local temperature with $\Delta t_f = 8 \times 10^5$, and (d) time average of wave number spectrum with $\Delta t_f = 8 \times 10^5$.

and 5(b) with $\Delta t_f = 1 \times 10^5$. The local temperature is lower than the applied temperature. The mean amplitude $A(\xi)$ of large wave numbers is lower than the average value. Too frequent clearance of high frequency modes does not leave enough time for them to grow. A longer filtering time $\Delta t_f = 8 \times 10^5$ gives results displayed in Figs. 5(c) and 5(d). The local temperature is higher than the applied temperature, and the mean amplitude $A(\xi)$ of large wave numbers is higher than the average value.

We observe that the filter clears energy in high frequency modes and balances the spurious growth due to numerical instability of the Runge-Kutta algorithm. The numerical tests validate the effectiveness, while the choice of the filtering time is empirical.

V. DISCUSSIONS

When used as an integrator for a linear harmonic chain, the second order Runge-Kutta algorithm is unstable for any time step size. The accumulation of energy appears more severe at larger time step size, and at larger wave number. Numerical tests and analyses reveal that this instability persists in the numerical integration of the Nosé-Hoover heat bath for a linear harmonic chain, while the interplay between instability and nonlinearity leads to a different growth rate. This understanding for the incompetency of the Runge-Kutta algorithm is further verified by a stabilization method via filter.

We remark that for higher order Runge-Kutta algorithms the numerical instability may be explored in a similar way, yet appears even weaker. An even longer filtering time may be chosen. This may explain the seemingly stable numerical results in [26], where a linear harmonic chain was simulated by an eighth order Runge-Kutta algorithm. They also reported indefinite growth of temperature for longer-time calculations [38]. From this paper, we discover that the linear instability of the Runge-Kutta algorithm is the underlying reason.

ACKNOWLEDGMENTS

This research is partially supported by National Natural Science Foundation of China under Grants No. 11521202 and No. 11272009. We would like to thank Dr. Jianjin Wang for stimulating discussions.

[1] H. C. Anderson, J. Chem. Phys. **72**, 2384 (1980).
[2] H. J. C. Berendsen, J. P. M. Postma, W. F. van Gunsteren, A. DiHola, and J. R. Haak, J. Chem. Phys. **81**, 3684 (1984).
[3] G. Bussi and M. Parrinello, Phys. Rev. E **75**, 056707 (2007).
[4] S. Nosé, J. Chem. Phys. **81**, 511 (1984).
[5] W. G. Hoover, Phys. Rev. A **31**, 1695 (1985).
[6] E. G. Karpov, H. S. Park, and Wing Kam Liu, Int. J. Numer. Meth. Eng. **70**, 351 (2007).

[7] S. Tang and B. Liu, Commun. Comput. Phys. **18**, 1445 (2015).
[8] B. Liu and S. Tang, Comput. Mech. **59**, 843 (2017).
[9] G. J. Martyna, M. L. Klein, and M. Tuckerman, J. Chem. Phys. **97**, 2635 (1992)
[10] D. Janezic, and B. Orel, J. Chem. Inf. Comput. Sci. **33**, 252 (1993).
[11] M. P. Allen and D. L. Tildesley, *Computer Simulations of Liquids* (Clarendon, Oxford, 1987).
[12] M. Tuckerman, B. J. Berne, and G. J. Martyna, J. Chem. Phys. **97**, 1990 (1992)
[13] T. Mai, A. Dhar, and O. Narayan, Phys. Rev. Lett. **98**, 184301 (2007).
[14] D. Xiong, Y. Zhang, and H. Zhao, Phys. Rev. E **90**, 022117 (2014).
[15] A. Dhar and K. Saito, Phys. Rev. E **78**, 061136 (2008).
[16] D. Xiong, Y. Zhang, and H. Zhao, Phys. Rev. E **88**, 052128 (2013).
[17] T. Sun, J. Wang, and W. Kang, Europhys. Lett. **105**, 16004 (2014).
[18] T. Sun, J. Wang, and W. Kang, Nanoscale **5**, 128 (2013).
[19] W. R. Zhong, M. P. Zhang, B. Q. Ai, and D. Q. Zheng, Appl. Phys. Lett. **98**, 113107 (2011).
[20] J. Shiomi and S. Maruyama, Jpn. J. Appl. Phys. **47**, 2005 (2008).
[21] S. Tsuzuki, H. Matsumoto, W. Shinoda, and M. Mikami, Phys. Chem. Chem. Phys. **13**, 5987 (2011).
[22] K. Laasonen and M. L. Klein, J. Chem. Soc., Faraday Trans. **91**, 2633 (1995).
[23] A. Suenaga, C. Yatsu, Y. Komeiji, M. Uebayasi, T. Meguro, and I. Yamato, J. Mol. Struct. **526**, 209 (2000).
[24] S. Lepri, R. Livi, and A. Politi, Phys. Rep. **377**, 1 (2003).
[25] S. Lepri, R. Livi, and A. Politi, Phys. Rev. Lett. **78**, 1896 (1997).
[26] B. Hu, B. Li, and H. Zhao, Phys. Rev. E **61**, 3828 (2000).
[27] A. Lippi and R. Livi, J. Stat. Phys. **100**, 1147 (2000).
[28] B. Li, H. Zhao, and B. Hu, Phys. Rev. Lett. **86**, 63 (2001).
[29] R. Su, Z. Yuan, J. Wang, and Z. Zheng, Phys. Rev. E **91**, 012136 (2015)
[30] B. Q. Ai and B. Hu, Phys. Rev. E **83**, 011131 (2011).
[31] A. V. Savin and O. V. Gendelman, Phys. Rev. E **67**, 041205 (2003).
[32] A. Ueda and S. Takesue, J. Phys. Soc. Jpn. **75**, 044003 (2006).
[33] Y. Zhong, Y. Zhang, J. Wang, and H. Zhao, Phys. Rev. E **85**, 060102(R) (2012).
[34] K. Feng, J. Comput. Math. **4**, 279 (1986).
[35] K. Feng and M. Qin, *Symplectic Geometric Algorithms for Hamiltonian Systems* (Zhejiang, Hangzhou, 2010).
[36] M. P. Calvo and J. M. Sanz-Serna, SIAM J. Sci. Comput. **14**, 936 (1993).
[37] E. Hairer and G. Wanner, *Solving Ordinary Differential Equations* (Springer, New York, 1996), Vol. 2.
[38] H. Zhao and J. Wang (private communication).